Available online at www.sciencedirect.com
ScienceDirect
Tetrahedron
Tetrahedron 62 (2006) 10237–10247

Structure, intramolecular flexibility, and complexation of aza crown ethers to anions $H_2PO_4^-$ and HSO_4^- in nonprotic solvents

Erich Kleinpeter* and Anja Holzberger

Chemisches Institut, Universität Potsdam, PO Box 60 15 53, D-14415 Potsdam, Germany

Received 19 June 2006; revised 14 July 2006; accepted 25 July 2006
Available online 7 September 2006

Abstract—Both the structure and intramolecular flexibility of a series of aza crown ethers were studied by experimental NMR and theoretical molecular modeling. The stoichiometries of complexation to the anions $H_2PO_4^-$ and HSO_4^- and resulting complex stabilities were determined by experimental NMR (^1H, ^{31}P) titration and, in addition, the structure and mobility changes of the aza crown ethers upon complexation were also examined.

1. Introduction

The use of aza crowns for anion complexation is a long standing classic of supramolecular chemistry, starting with the early papers of Hosseini and Lehn.[1] A number of reviews of this research have been published.[2] Aza crown ethers due to their nitrogen lone pairs and N–H moieties are potentially able to complex both cations and anions, dependent on the pH value of aqueous solution. This kind of research is still popular because of the continuing search for useful sensor systems.

Just recently two papers were published studying not only the ability of this kind of compounds for their complexation to Cu^{2+}, Hg^{2+}, and Ni^{2+},[3] but also dealing, at the same time, with the ability of certain aza crowns to coordinate to certain anions in aqueous solution.[4] Although a number of X-ray structures of the complexes have been reported,[5] only limited information is available on the conformation of both aza crown ether hosts and their complexes in solution: Novak and Potts[6] have determined by photoelectron spectroscopy the cavity width of 12-tetraaza crown-4 ether (**1**) and 14-tetraaza crown-4 ether (**4**); Ranganathan et al.[7] detailed the vicinal H,H couplings of 12-tetraaza crown-4 ether (**1**) with respect to the preferred conformation of the compound and found that *synclinal* N–C–C–N fragments were well preorganized for complexation. At the same time, Bultinck et al.[8] ab initio MO calculated at the HF level the latter compound and confirmed the *synclinal* N–C–C–N conformations and, in addition, determined that hydrogen bonding plays only a minor role in stabilizing the ground state geometry of 14-tetraaza crown-4 ether (**4**) and its analogs in solution. Rather than hydrogen bonding, it is the electrostatic repulsions of the N-lone pairs that are determinate for the global minima states.

In addition to the aforementioned tetraaza crown ethers, we have synthesized a series of analogs (Scheme 1) and studied both experimentally by NMR and theoretically by molecular modeling with respect to their preferred conformers. The flexibility of both the free entities and when complexed to the anions $H_2PO_4^-$ and HSO_4^- was also evaluated as was the stoichiometry and stability of the complexes.

2. Results and discussion

2.1. NMR spectra

The ^1H and ^{13}C NMR spectra of the compounds were consistent with the structures presented in Scheme 1 and the nuclei absorb in the ranges expected (see Tables 1 and 2). From both ^1H and ^{13}C NMR spectra, due to the number of observed lines, it can be concluded that the compounds are symmetric on the NMR timescale although lines in both spectra were somewhat broadened and thus restricted interconversion of the macrocyclic rings or some other slow process in the compounds is inferred.

2.2. Complexation study

In order to test the complexational behavior of the di-, tri-, and tetraaza crown ethers **1**–**10** to anions, NMR titration experiments with the salts $H_2PO_4^-{}^+N(n\text{-Bu})_4$ and $HSO_4^-{}^+N(n\text{-Bu})_4$ were performed in $CDCl_3$. Both the ^1H

Keywords: Conformational analysis; Aza crown ethers; Anion complexation; Stoichiometry; Spin–lattice relaxation times T_1.
* Corresponding author. Tel.: +49 331 977 5210; fax: +49 331 977 5064; e-mail: kp@chem.uni-potsdam.de

0040–4020/$ - see front matter © 2006 Elsevier Ltd. All rights reserved.
doi:10.1016/j.tet.2006.07.074

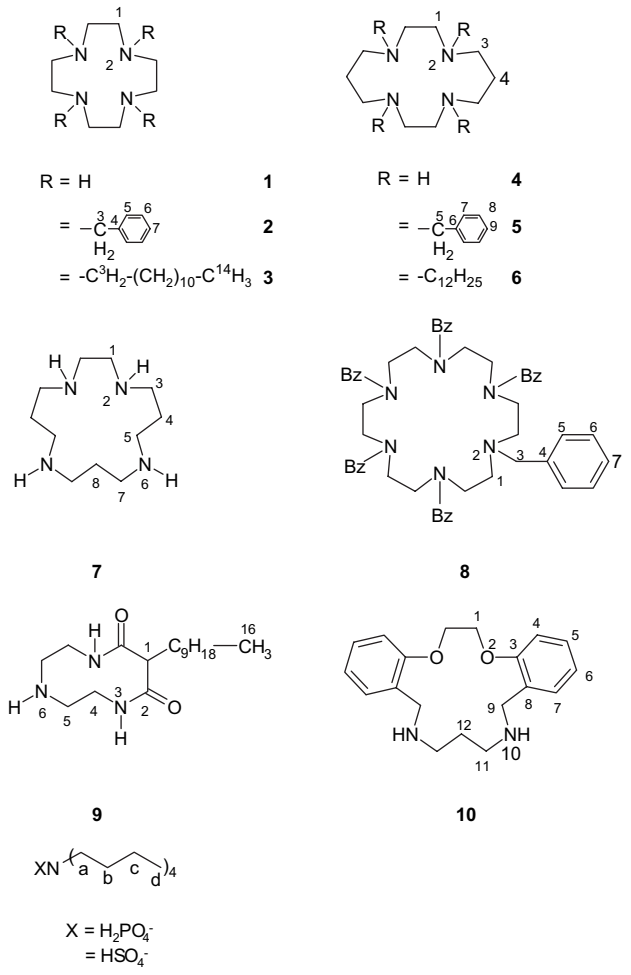

Scheme 1. Compounds studied.

and ^{13}C chemical shifts of the various nuclei were followed with increasing addition of the anions and, in case of the phosphate titration, the ^{31}P NMR was also recorded.[9] With increasing amounts of anion, both the ^{1}H and ^{13}C chemical shifts of the macrocyclic ring atoms as well as those of the R substituents were shifted, and thus complexation was evident. The same conclusion was drawn from the behavior of the ^{31}P chemical shifts in the case of phosphate anion. The stoichiometry of the complexes was determined from Job's plots,[10] e.g., Figure 1 illustrates the titration of **9** with $H_2PO_4^-{}^+N(n\text{-}Bu)_4$ following the ^{1}H chemical shift changes of several protons as well as of the ^{31}P signal of the added salt.

With respect to the stoichiometry of the complexes, the following results were obtained: (i) complexes between dioxa,diaza crown ether **10** and $H_2PO_4^-$ and between hexaaza crown ether **8** and HSO_4^- do not form at all, (ii) the unsubstituted tetraaza crown ethers **1** and **4** form 1:2 complexes with phosphate, due to dimerization of $H_2PO_4^-$ by hydrogen bonding in the less polar solvent $CDCl_3$,[11] (iii) 1:1 complexation occurs in the case of **2**, **3**, and **5**–**9** with $H_2PO_4^-$, and (iv) all of the crown ethers studied, except for **8**, form 1:1 complexes with HSO_4^-. The stability constants of the complexes are presented in Table 3 and lie in the range 1.21–4.91 for log *K*. Similar values were obtained by Martell et al.[12] for the coordination of $H_2PO_4^-$ with dioxa,hexaaza macrocycles in aqueous solution. The lowest complexation for $H_2PO_4^-$ and HSO_4^- was obtained for **3**; obviously, due to the long fatty acid tails the macrocyclic ring system is sterically hindered and thus limits anion complexation. The *N*-unsubstituted tetraaza crown ethers **1**, **4**, and **7** are the most useful for complexing the selected anions as complexation constants of log $K>3$ were obtained. If complexation of the aza crown ethers is compared with respect to both their ring size and substitution, the following orders are obtained: with respect to ring size, **1**>**4** and **2**>**5**; and with respect to substitution, R=H>R=benzyl>R=alkyl. The lowest tendency for complexation was observed for **3** and **6** due to the previously mentioned steric hindrance; the less flexible benzyl substituents in **2** and **5**, however, allow easier approach of the anions to the host cavity for successful complexation.

2.3. Structural information from ^{1}H and ^{13}C NMR spectra

Structural information was limited due to fast ring interconversion at ambient temperature and, further, the symmetry of the aza crown ethers.

2.3.1. *J* information. The weighted averages of the participating *synclinal*, *anticlinal* and *antiperiplanar* conformations change with increasing steric hindrance (cf. Table 4) and thus changes in the $^{3}J_{H,H}$ values, when measurable, imply variations in the dihedral angles N–C–C–C. For **4** (an unsubstituted aza crown), the optimal conformer is *synclinal*, but in **5**, and even more so in **6**, this dihedral angle changes evermore to the *anticlinal* conformation due to the steric hindrance of the R substituents. Similar $^{3}J_{H,H}$ values were obtained for both the free and the complexed crown ethers, and so obviously complexation does not very much change the conformational equilibria of the host compounds (as far as it could be concluded from weighted averages in $^{3}J_{H,H}$)—thus, **4** and **7** seem to be already in free state well organized for complexation.

2.3.2. Spatial information. Only limited NOE spatial information was obtained for **2**, **5**, and **8** (NOE contacts were not observed in the NOESY/ROESY spectra obtained for **1**, **3**, **4**, **6**, **7**, and **9**). NOEs between the NCH_2 and *ortho* phenyl protons were observed, however, this is without structural implication. The situation improves slightly in **10** where NOEs between H-1···H-4, H-7···H-9, and H-9···H-11 were observed and thus some dihedral angles can be excluded: NOE (H-1···H-4) indicates the *antiperiplanar* or *anticlinal* conformation of C_1–O_2–C_3–C_7; NOE (H-7···H-9) is representative for *synclinal* or *anticlinal* conformation of C_7–C_8–C_9–N_{10} (*synperiplanar* arrangement precludes NOEs and the *antiperiplanar* conformer is sterically prevented); and NOE (H-9···H-11) provides an indication of the geometry of the C_8–C_9–N_{10}–C_{11} and O_2–C_1–$C_{1'}$–$O_{2'}$ systems. Only if the C–C–N–C moiety is in a *synclinal* arrangement the two protons H-9 and H-11 can remain within a measurable NOE distance for each orientation of the other C–C–N–C dihedral angle. Finally, O_2–C_1–$C_{1'}$–$O_{2'}$ must be in a *synclinal* or *anticlinal* orientation as an *antiperiplanar* orientation would bring H-1 near to H-2, an NOE contact, which was not detected.

Of note, intermolecular NOEs were also measured between host protons and those of the $^{+}N(n\text{-}Bu)_4$ ammonium cation.

Table 1. ^{1}H NMR chemical shifts (δ/ppm) of the aza crown ethers **1–10** and differential values upon complexation to $H_2PO_4^-$ and HSO_4^- anions

Compound	H-1	N(2)H	H-3	H-4	H-5	H-6	H-7	H-8	H-9	H-10	H-11	H-12	H-13	H-14	H-15	H-16
1	2.65	2.56		—	—	—	—	—	—	—	—	—	—	—	—	—
1···$H_2PO_4^-$	−0.13															
1···HSO_4^-	+0.03															
2	2.68		3.43		7.36	7.25	7.19									
2···$H_2PO_4^-$	−0.02		−0.01		−0.01	−0.01	+0.01									
2···HSO_4^-	+0.06		+0.03		+0.03	+0.07	+0.12									
3	3.51		2.30	1.64	1.27									0.89		
3···$H_2PO_4^-$	−0.06		−0.02	−0.01	−0.02									−0.01		
3···HSO_4^-	−0.12		+0.08	+0.07	+0.09									+0.09		
4	2.66	3.35	2.73	1.7												
4···$H_2PO_4^-$	−0.16		−0.06	−0.04												
4···HSO_4^-	−0.39	−0.45	+0.01	+0.02												
5	2.59		2.49	1.73	3.42		7.29	7.24	7.18							
5···$H_2PO_4^-$	−0.06		−0.04	−0.15	−0.05		−0.09	−0.07	−0.07							
5···HSO_4^-	+0.03		+0.03	+0.02	+0.03		+0.07	+0.02	±0							
6	2.65		2.88	1.40	2.32	1.26										0.88
6···$H_2PO_4^-$	−0.02		+0.04	+0.05	+0.01	−0.03										−0.03
6···HSO_4^-	±0		+0.05	+0.08	+0.04	±0										+0.11
7	2.67	2.97	2.71	1.67	2.71	2.97	2.71	1.70								
7···$H_2PO_4^-$	−0.12		−0.06	−0.02	−0.06		−0.06	−0.05								
7···HSO_4^-	+0.16		+0.12	+0.15	+0.12		+0.12	+0.12								
8	3.13		3.42		7.06	7.34	7.41									
8···$H_2PO_4^-$	−0.05		+0.19		−0.05	−0.14	−0.03									
8···HSO_4^-	[a]															
9	4.19		1.83	3.32	2.76	1.83	1.83	1.24								0.87
9···$H_2PO_4^-$	−0.44		−0.08	+0.27	+0.13	−0.08	−0.08	+0.01								−0.01
9···HSO_4^-	−0.49		−0.07	+0.23	+0.34	−0.07	−0.07	−0.02								±0
10	4.39			6.92	6.89	7.29	7.20		3.75	1.91	2.64	1.75				
10···$H_2PO_4^-$	[a]															
10···HSO_4^-	−0.04			+0.30	+0.32	+0.01	+0.08		+0.17		+0.09	−0.11				

[a] No coordination observed.

Obviously, not only the anion, but also the cation (as a salt pair) forms part of the complexes. Similar suggestions have been made by Valiyaveettil et al.[11] when studying the phosphate complexation of open-chain polyaza ethylene compounds. Actually, evidence for the existence of such complete complexes was implied by ESIMS measurements.[13]

2.4. Flexibility information from T_1 measurements

Spin–lattice relaxation times T_1 of certain aza crown ether protons were measured in order to confirm the interaction of the aza crown ethers with the two different anions (cf. Table 5). As expected, with increasing amounts of the two different anions in solution, the T_1s were reduced in value. This is due to complexation in reducing the intramolecular flexibility of the aza crown ethers.[14]

The T_1s of the NCH_2 protons of the ammonium cations were also measured (see Table 6), and these values proved to be very interesting since the cations are not directly involved in aza crown ether···anion complexation. In the case of the *N*-unsubstituted tetraaza crowns **1**, **4**, and **7**, the T_1s increased in value leading to the conclusion that as the anion complexes with the aza crown ethers, ammonium cations are less strongly bound to the anion (as ion pairs) and their flexibility therefore increases. In the remaining aza crowns **2**, **3**, **5**, **6**, and **8–10**, complexation to the anion was only minor or non-existent, therefore no effect on the T_1 values of the ammonium cation protons was expected and they should remain constant. However, they were observed to decrease in value and the only conclusion from this result is that obviously the long fatty acid chains attached to the aza crown ethers and the *n*-butyl chains of the ammonium cation become arranged along each other due to hydrophobic interactions and thereby the flexibility of the ammonium cation is reduced and subsequently the T_1 values decrease as well.

2.5. Variable temperature ^{1}H and ^{13}C NMR spectroscopy

Since some signals of the aza crown ethers in both the ^{1}H and ^{13}C NMR spectra were already broadened at ambient temperature, deconvolution was thus expected at lower temperatures and the aza crown solutions, both free as well as complexed to phosphate and sulfate, were examined accordingly. However, only in case of **10** this was successful. This dioxa,diaza crown ether contains some rigid units, which reduce the flexibility of the macrocyclic 15-membered ring system (vide supra) and from following the line width of H-1 and H-9, the free energy of interconversion of the 15-membered ring could be calculated to be 9.2–9.3 kcal/mol, in excellent agreement with values obtained for similar crown ethers.[15]

The ring interconversion of the remaining aza crown ethers **1–9** could not be frozen within the temperature range of the present NMR equipment when observing ^{1}H NMR spectra.

Table 2. ^{13}C NMR chemical shifts (δ/ppm) of the aza crown ethers **1–10** and differential values upon complexation to $H_2PO_4^-$ and HSO_4^- anions

Compound	C-1	N-2/C-2	C-3	C-4	C-5	C-6	C-7	C-8	C-9	C-10	C-11	C-12	C-13	C-14	C-15	C-16
1	46.5															
1···$H_2PO_4^-$	−0.9															
1···HSO_4^-	+0.5															
2	53.0		60.1	140.1	128.9	128.0	126.6									
2···$H_2PO_4^-$	−0.4		−0.5	+0.6	−0.1	−0.1	−0.1									
2···HSO_4^-	+0.3		+0.6	−11.0	+1.3	+2.2	+2.2									
3	49.9		31.9	29.6	25.3	22.7[a]								14.1		
3···$H_2PO_4^-$	−0.6		±0	+0.1	−0.1	±0										
3···HSO_4^-	−0.2		+0.1	+0.2	±0	±0										
4	50.8		49.3	29.3												
4···$H_2PO_4^-$	−1.6		+1.3	±0												
4···HSO_4^-	−1.5		+1.4	+1.4												
5	50.8		51.9	24.4	59.6	140.6	129.8	128.6	127.6							
5···$H_2PO_4^-$	−0.4		−0.5	−0.3	−0.2	−0.6	−0.9	−0.6	−1.0							
5···HSO_4^-	+0.5		+0.5	+0.2	+0.7	+0.3	+0.1	+1.0	+0.1							
6	62.0		56.2	31.9	32.2	14.1	29.6	28.0	23.4[a]							
6···$H_2PO_4^-$	−0.6		+2.3	+1.6	−0.4	−0.1	+1.2	−0.8	±0							
6···HSO_4^-	−2.2		−1.8	+0.2	−0.3	±0	+1.4	−0.7	±0							
7	49.5		49.8	28.8	50.4		51.3	29.2								
7···$H_2PO_4^-$	−0.5		−0.8	±0	−0.6		−1.2	+0.1								
7···HSO_4^-	+1.8		+0.4	+2.1	+0.2		±0	+0.9								
8	48.5		59.5	139.1	129.8	128.5	132.8									
8···$H_2PO_4^-$	−0.2		−1.9	−0.4	−0.7	−1.2	−2.5									
8···HSO_4^-	[b]															
9	61.5	171.1		39.2	47.8		29.6, 14.1	29.3	22.7[a]							
9···$H_2PO_4^-$	−2.4	−0.7					+0.1	+0.1	±0	±0						
9···HSO_4^-	−1.7	−0.6					+0.1	+1.4	+0.8	+0.1						
10	65.7		158.2	110.1	120.6	128.5	131.2	158.2	51.6		47.8	29.0				
10···$H_2PO_4^-$	[b]															
10···HSO_4^-	−0.2		+0.8	+0.1	±0	+0.8	+0.9	+0.8	+1.6		+0.8	−3.5				

[a] Not further assigned.
[b] No coordination observed.

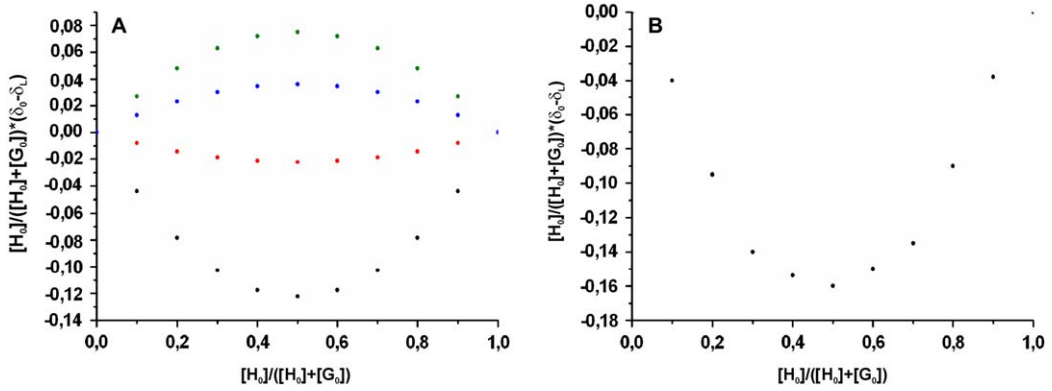

Figure 1. Job plots of the titration of **9** with $H_2PO_4^-$: (A) ^1H NMR and (B) ^{31}P NMR chemical shift variations; from the plot of the two parameters the anion-to-ligand ratio of the complexes was inferred by the value of the *x*-coordinate at the plot azimuth.

Table 3. Stability constants and stoichiometry of the complexes of **1–10** (log *K*) with $H_2PO_4^-$ and HSO_4^- anions

Complex	**1**	**2**	**3**	**4**	**5**	**6**	**7**	**8**	**9**	**10**
With $H_2PO_4^-$	4.67	2.52	1.68	3.40	2.18	2.08	3.30	2.19	4.91	[a]
	1:2	1:1	1:1	1:2	1:1	1:1	1:1	1:1	1:1	—
With HSO_4^-	3.53	2.31	1.21	3.23	2.55	2.17	3.89	[a]	4.40	2.83
	1:1	1:1	1:1	1:1	1:1	1:1	1:1	—	1:1	1:1

[a] No coordination observed.

Table 4. $^3J_{H,H}$ coupling constants (Hz) in free aza crown ethers **4–7** and **10** and in their complexes with $H_2PO_4^-$ and HSO_4^- anions

Compound	Free	With $H_2PO_4^-$	With HSO_4^-
4	5.5	5.0	5.5
5	7.0	7.0	7.0
6	8.5	8.5	8.0
7	5.0	5.0	5.0
10	5.5	[a]	5.5

[a] No coordination observed.

Table 5. Spin–lattice relaxation times T_1 (s) of the H-1 protons in aza crown ethers **1–10** and differential values in their complexes with $H_2PO_4^-$ and HSO_4^- anions

Compound	**1**	**2**	**3**	**4**	**5**	**6**	**7**	**8**	**9**	**10**
Free crown	1.1	0.4	0.35	1.0	0.4	0.3	0.9	0.4	0.6	0.7
$+H_2PO_4^-$	−0.2	−0.05	−0.1	−0.1	−0.1	−0.05	−0.05	−0.05	−0.1	[a]
$+HSO_4^-$	−0.1	−0.05	−0.05	−0.1	−0.1	−0.05	−0.1	[a]	−0.1	−0.1

[a] No coordination observed.

Table 6. Spin–lattice relaxation times T_1 (s) of the NCH_2 protons of the ammonium cations and differential values upon complexation to aza crown ethers **1–10**

Compound	Free	Complexed									
		1	**2**	**3**	**4**	**5**	**6**	**7**	**8**	**9**	**10**
TBAHP[a]	0.2	+0.15	−0.1	−0.1	+0.1	−0.05	−0.05	+0.1	−0.15	−0.1	[b]
TBAHS[c]	0.25	+0.1	−0.1	−0.05	+0.05	−0.1	−0.05	+0.05	[b]	−0.1	−0.15

[a] Tetra-*n*-butyl ammonium hydrogen phosphate.
[b] No coordination observed.
[c] Tetra-*n*-butyl ammonium sulfate.

The signals broadened and split into overlapping, very wide absorptions on going down to 190 K but, due to these difficulties, barriers to ring interconversions could not be determined. For example, in Figure 2 the temperature dependence of the ^{1}H NMR spectrum of **2** is depicted.

Since the signal disparities in the corresponding ^{13}C spectra after deconvolution are generally larger than in the ^{1}H spectra and thus coalescence temperatures are usually higher,[14] the temperature dependence of the ^{13}C NMR signals was also examined, but again without success (cf. also Fig. 2). Even at 170 K the resonances did not decoalescence and only became more broadened. Thus, the line broadening as obtained must be, at least partly, assigned to the obviously complicated T_2 relaxational behavior of the aza crowns studied.[15b] The same result was obtained for the corresponding complexes and thus supports the aforementioned conclusion. The inherent broad width of the ^{1}H NMR signal lines also precluded the extraction of precise J information for conformational analysis and thus the accompanying molecular modeling study was necessary in order to overcome the deficiencies regarding the adopted conformations.

2.6. Molecular modeling of aza crown ethers 1–10 and their complexes

In order to assess the conformational behavior of **1–10**, the steric hindrance of the coordinating anions and the mechanism of complexation of the aza crown ethers and their anion complexes were also studied theoretically in detail.

The modeling study was started by random search calculations to estimate the conformational equilibria in solution. For each crown ether, 10^5 cycles were calculated and up to

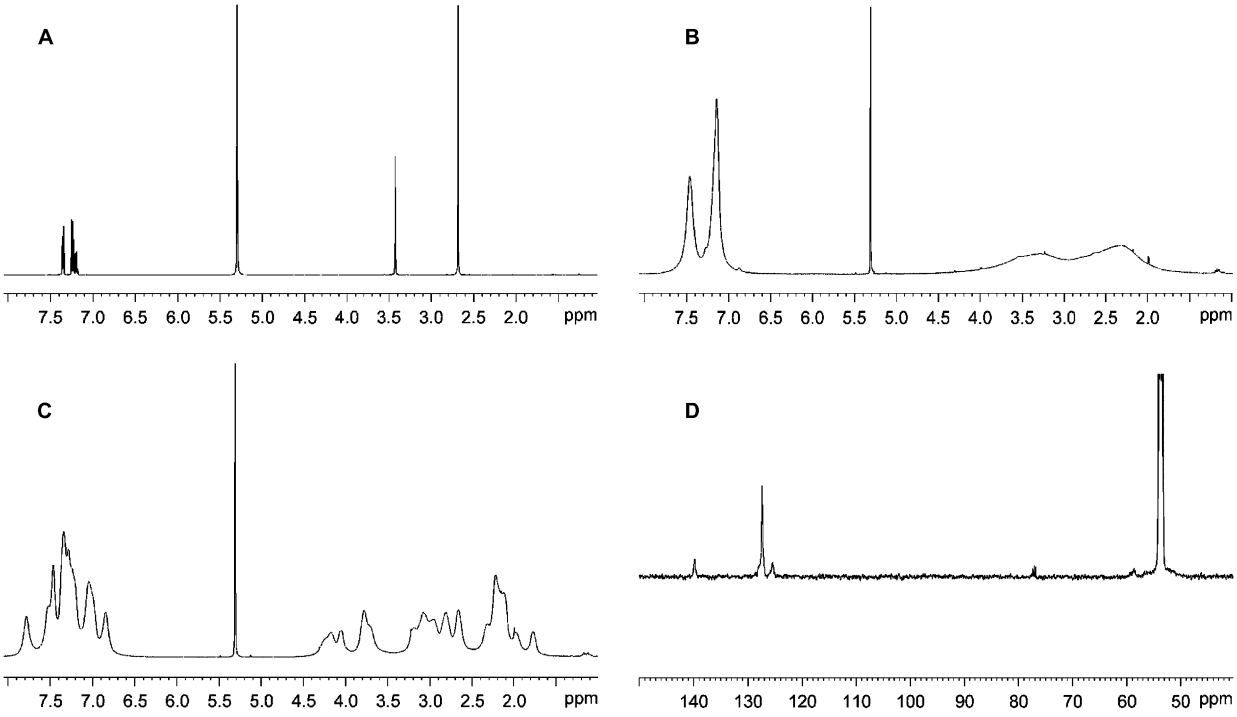

Figure 2. Temperature dependence of the NMR spectra of aza crown ether **2**: (A) ^{1}H at 298 K, (B) ^{1}H at 190 K, (C) ^{1}H at 170 K, and (D) ^{13}C at 170 K.

three torsional angles in the macrocyclic ring were varied *per* cycle and the obtained geometries were optimized by force field calculations. Conformations within 3 kcal/mol of the global minimum structure were stored in a data bank. However, in order to save CPU time the following simplifications were introduced: *N*-alkyl chains were substituted by *N*-methyl and the effect of the fatty acid tails was studied later by molecular dynamic simulations (vide infra); benzyl substituents were substituted by hydrogen but their effect later considered by grid search calculations and thus correct conformations of the benzyl substituted aza crowns could be obtained (vide infra).

The conformers obtained by the random search calculations were then continuum solvent geometry optimized by the PM3 method. Aza crown ethers **1** and **4** have already been ab initio MO studied by Bultinck et al.[8] and they were included into the present study in order to estimate the quality of the present semiempirical calculations.

As a result of this theoretical study, a large number of conformations were obtained within a relatively narrow energy window of 3 kcal/mol, though only the global minima structures of the various crowns were continuum solvent geometry optimized and collected in Table 7. Even if there is a number of different conformations for each aza crown ether studied, some really informative trends with respect to their ground state structures and complexational behavior can be construed:

(i) If the aza crown ethers are *N*-unsubstituted (**1**, **4**, **7**, and **9**), the macrocyclic ring with respect to the N–C–C–N dihedral angle is *synclinal* in orientation. This result is in complete agreement with both the theoretical studies of Wolf et al.[16] and Bultinck et al.[8]

(ii) If the aza crown ethers are *N*-substituted with the strong sterically hindering fatty acid tails or benzyl substituents, the corresponding N–C–C–N dihedral angles change from *synclinal* orientations to *antiperiplanar* and are seldom in *synclinal* or *anticlinal* orientations.

(iii) Adjacent C–N–C–C dihedral angles remain in a *synclinal* orientation, in good agreement with the NOE study of crown ether **10**.

(iv) The N–C–C–C torsional angles are in *synclinal* conformations, in agreement with experimental information (cf. **4** and **7**). The same *N*-substituent steric effect, as mentioned previously, is observed: N–C–C–C torsional angles change then to *antiperiplanar* conformations.

(v) Due to experimental data in the case of **10** ($^3J_{H_{11},H_{12}}$=5.5 Hz, no NOE between H-1 and H-11), the global minimum is validated: both the N–C–C–C and O–C–C–O torsion angles are *synclinal*, though *anticlinal* but not *antiperiplanar* conformations are also possible. In good agreement with the experiment results are the *anticlinal* C=C–C–N and C–O–C=C *antiperiplanar* conformations. The global minimum structure of dioxa,diaza crown ether **10** is presented in Figure 3.

2.7. Steric *N*-substituent effect on the conformation of the macrocyclic ring

Within this context, firstly, grid search calculations of the benzyl substituted aza crown ethers were processed. All

Table 7. Dihedral angles of the global minima structures of the aza crown ethers **1–10** as obtained by PM3 energy optimization

Compound	$NCCN^I$	CCN^IC	CN^ICC	N^ICCN^{II}	$CCN^{II}C$	$CN^{II}CC$	$N^{II}CCN^{III}$	$CCN^{III}C$	$CN^{III}CC$	$N^{III}CCN$	CCNC	CNCC
1	129	−79	142	−79	−85	73	68	−167	69	86	−83	−82
2	78	−97	−59	168	−69	−60	162	−57	−68	147	−155	64
3	165	−79	82	−152	62	69	−164	137	−88	120	−93	−60

Compound	NCCC	$CCCN^I$	CCN^IC^I	$CN^IC^IC^I$	$N^IC^IC^IN^{II}$	$C^IC^IN^{II}C^{II}$	$C^IN^{II}C^{II}C^{II}$	$N^{II}C^{II}C^{II}C^{II}$	$C^{II}C^{II}C^{II}N^{III}$	$C^{II}C^{II}N^{III}C^{III}$	$C^{II}N^{III}C^{III}C^{III}$	$N^{III}C^{III}C^{III}N$	$C^{III}C^{III}NC$	$C^{III}NCC$
4	−90	180	−137	55	66	−154	112	−168	83	91	−68	−77	172	−69
5	−179	−100	75	−160	76	68	−161	−170	−97	41	−95	−170	−80	−73
6	−159	−177	−67	84	−170	73	59	−177	148	−65	159	−110	−56	93
7	81	76	172	176	−80	79	63	−167	180	−78	−67	177	−69	−87

Compound		$NCCN^I$	CCN^IC	CN^ICC	N^ICCN^{II}	$CCN^{II}C$	$CN^{II}CC$	$N^{II}CCN^{III}$	$CCN^{III}C$	$CN^{III}CC$	$N^{III}CCN^{IV}$	$CCN^{IV}C$	$CN^{IV}CC$	$N^{IV}CCN^{V}$	$CCN^{V}C$	$CN^{V}CC$	$N^{V}CCN$	CCNC	CNCC
8	0.00	84	−86	168	−148	−63	179	−158	−57	139	−55	52	143	92	33	131	−159	−103	66
9	0.00	−147	60	48	−147	122	−62	99	−144	60	64	−123	74	159	−166	−85	84	−127	177

Compound		O^IC^ICO	C^ICCO	COCC	OCCC	CCCN	CCNC	CNCC	$NCCC^I$	CCC^IN^I	$CC^IN^IC^I$	$C^IN^IC^IC^I$	$N^IC^IC^IC^I$	$C^IC^IC^IO^I$	$C^IC^IO^IC^I$	$C^IC^IO^IC$
10	0.00	−59	−78	121	−8	103	−82	−53	−68	171	−71	115	118	1	168	−78

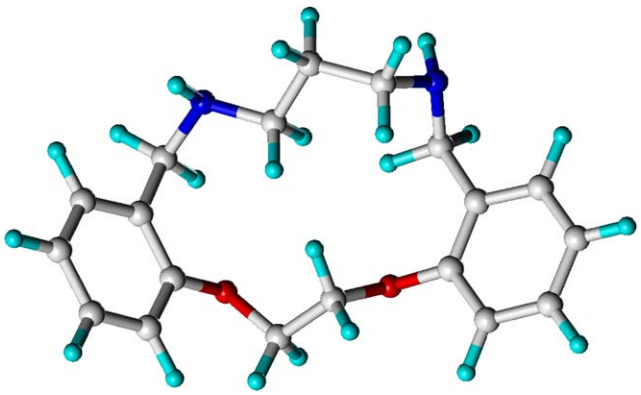

Figure 3. Global minimum structure of crown ether **10**.

the torsional angles C–N–C–C_{ar} and N–C–C_{ar}–C_{ar} were varied systematically in 30° steps and the structures thus obtained were energetically optimized. Comparing the resulting structures and their energies, it was clear that those conformations with *N*-benzyl substituents oriented exocyclically were the most stable ones. Thus, an *N*-benzyl substituent does not shield the aza crown cavity completely but allows the opportunity for anion complexation, and this is available from both sides of the macrocycle (cf. Fig. 4).

In order to consider the much more flexible fatty acid tails, molecular dynamic simulations were employed. For **3**, **6**, and **9**, the global minima structures from random search calculations were applied substituted with the corresponding *N*-alkyl chains (C-12 in the case of **3** and **6** but C-10 in the case of **9**). During 1 ns, the substituents were allowed to move freely at 300 K, the aza crown ether skeleton, however, was structurally fixed. The results are not surprising: the fatty acid tails sterically shield the macrocyclic ring cavity (cf. Fig. 5) to a great extent and thereby prevent the opportunity of the anions to approach for complexation. By contrast, the single $C_{10}H_{21}$ alkyl chains in aza crown ether **9** are unable to cover the whole macrocyclic ring cavity (cf. Fig. 6). They can partly cover one side of the cavity, but only one and thus from the opposite side the approach of the anion is possible and hence complexation with adequate complex stability results (vide supra).

2.8. Host–guest interaction in the $H_2PO_4^-$ and HSO_4^- complexes

Various models concerning the present host–guest interactions have been published. Lu et al.[17] consider the number and strength of potential hydrogen bondings as the fundamental criterion for successful complexation—complex stability increases if aza crown ethers are protonated.[15] Albelda et al.,[18] on the other hand, suggest that $H_2PO_4^-$ should be sufficiently acidic to protonate nitrogen atoms (the corresponding ^{15}N chemical shifts are strongly deshielded by complexation) and complex to the aza crown ethers via

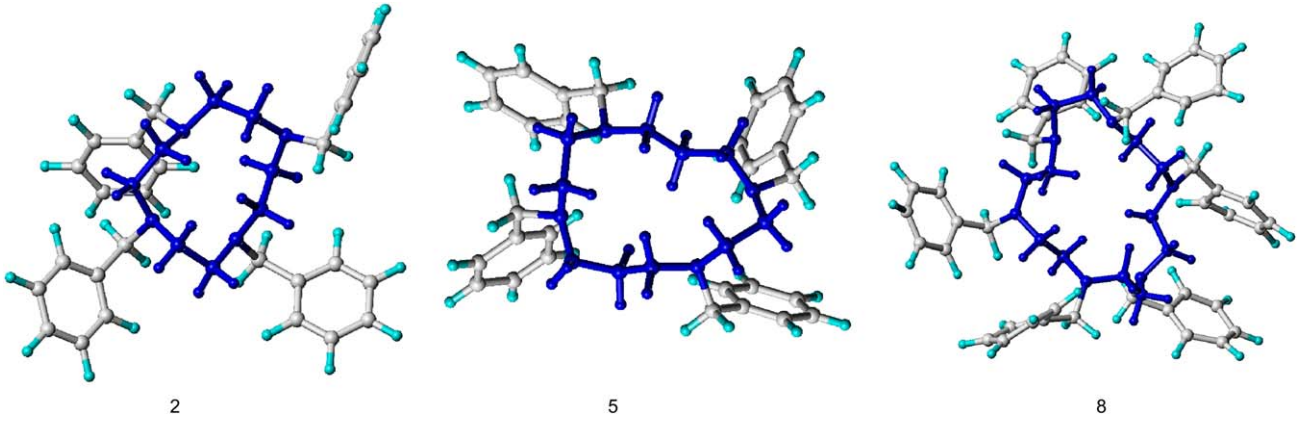

Figure 4. Preferred ground state conformations of aza crown ethers **2**, **5**, and **8**.

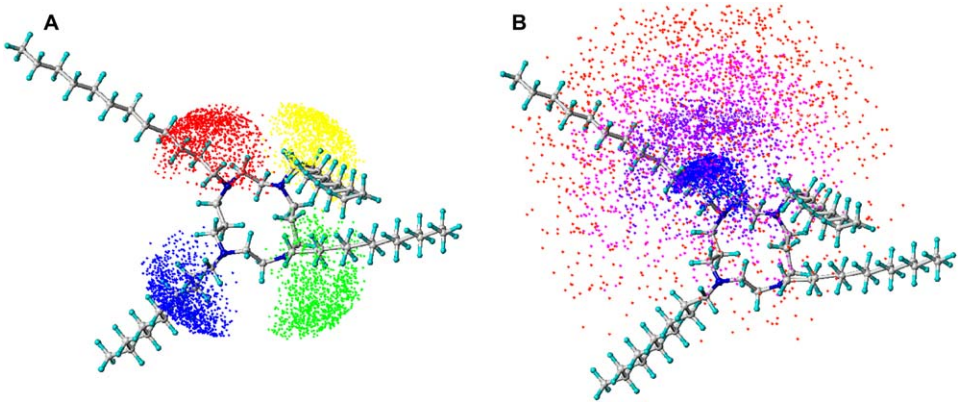

Figure 5. Spatial extension of fatty acid tails in crown ether **6**; possible positions of C-8 (A) and mobility of the alkyl chain (B).

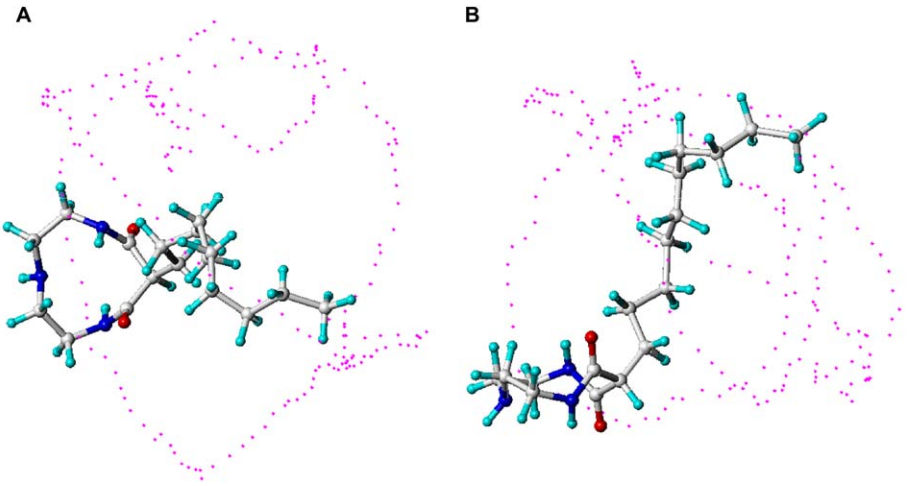

Figure 6. Mobility of the single alkyl chain of crown ether **9** illustrated from two different directions (A and B).

electrostatic interactions. And finally, Beer and Gale[19] consider that the charged anions can complex to the neutral aza crown ethers via dipole–ion interactions.

Firstly, hydrogen bonding was examined: the anions $H_2PO_4^-$ and HSO_4^- were positioned near to the cavity (P═O and S═O moieties, respectively, in the direction of the cavity) of the NH aza crown ethers **1**, **4**, **7**, **9**, and **10** and then PM3 geometry was optimized. The following trend was evident: P═O and NH of the aza crown ether form hydrogen bonds (cf. Fig. 7 for aza crown ether **1**) and the macrocyclic ring changes its conformation in order to enable as many of these hydrogen bonds as possible, at the same time, the anion occupies the most favorable position possible. However, the aza crown cavity cannot completely host the entire anion as has been observed for 20-membered rings[18] because of the smaller ring sizes in **1**–**10**. If the aza crown ethers studied are *N*-substituted (**2**, **3**, **5**, **6**, and **8**) then the former interaction (hydrogen bonding), however, is excluded.

In order to study possible N-protonation of the ligand by the anion, the relevant ligands were monoprotonated and a HPO_4^{2-} species was positioned near to the cavity and this geometry was then optimized. The result of this approach is obvious (cf. Fig. 8 for N-protonation of $\mathbf{3}H^+$—instead of the long alkyl chains only R=Me was considered): the NH proton left the crown ether moiety and transferred back to the oxygen of the anion, but at the same time the anion approached the aza crown macrocyclic ring system to complete the complexation. Certainly hydrogen bonding could not be identified in these cases as a major source of stabilization and therefore dipolar-ion interaction was deemed to be the major source.

As the other mode for complex formation, dipole–ion interactions were further considered. On the Connolly surface[20] of the aza crown ethers (generated by SYBYL)[21] surrounded by the solvent, the electrostatic potential[22] of the aza crown ethers was projected and the anion positioned near the positive charge region (cf. Fig. 9 for aza crown ether 2—instead of benzyl only R=Me was considered). Geometry optimization resulted in the following: N–C–C–N dihedral angles changed completely to *antiperiplanar* positions and the NCH_2 groups pointed to the inside of the macrocyclic ring system. Both P═O and S═O anion moieties also pointed to the same direction but the N-lone pairs are positioned away from the anion, obviously in order to minimize the repulsion of anion negative charges and N-lone pairs. In the case of this kind of conformation, already present in the starting structures, nothing changes during the energy minimization of the complexes. During the approach of the anion, the electron density of the phosphate/sulfate protons is shifted to other parts of the anion; the electrostatic potential of the aza crown near to the P═O/S═O bonds demonstrates the large positive range of the aza crown ethers in this respect (cf. the red area of Fig. 9).

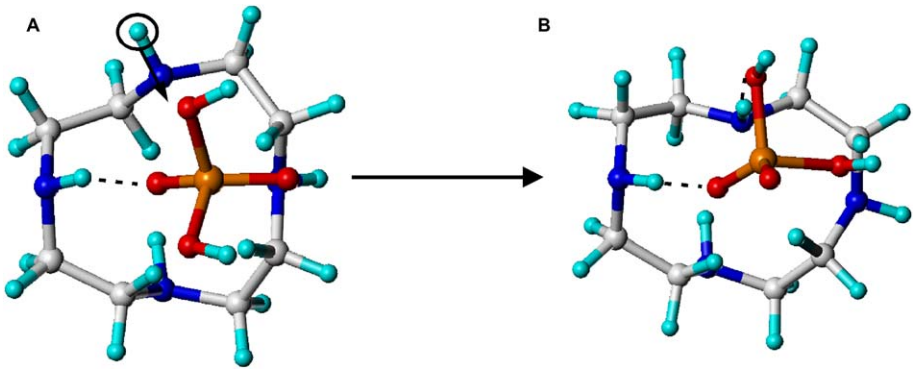

Figure 7. PM3 optimized geometry of the host–guest complex $\mathbf{1}\cdots H_2PO_4^-$ (A) before and (B) after optimization.

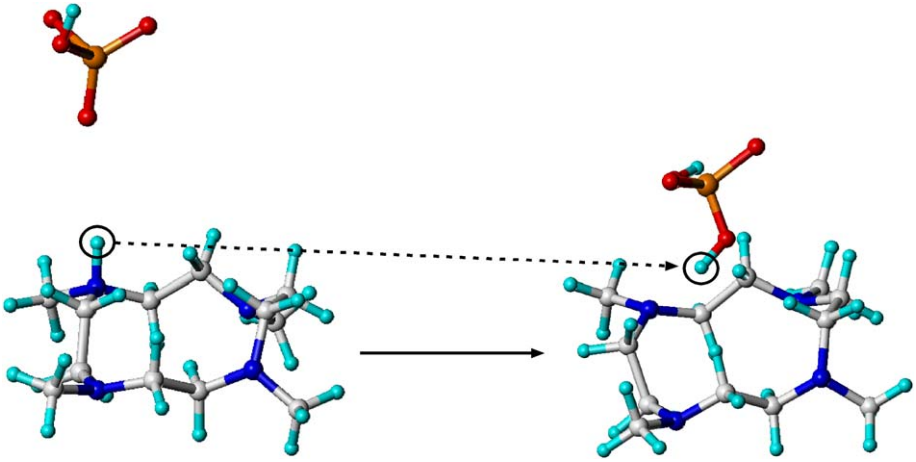

Figure 8. PM3 energy optimization of the $\mathbf{3}H^{+}\cdots HPO_4^{2-}$ complex—instead of the long alkyl chain only R=Me was considered.

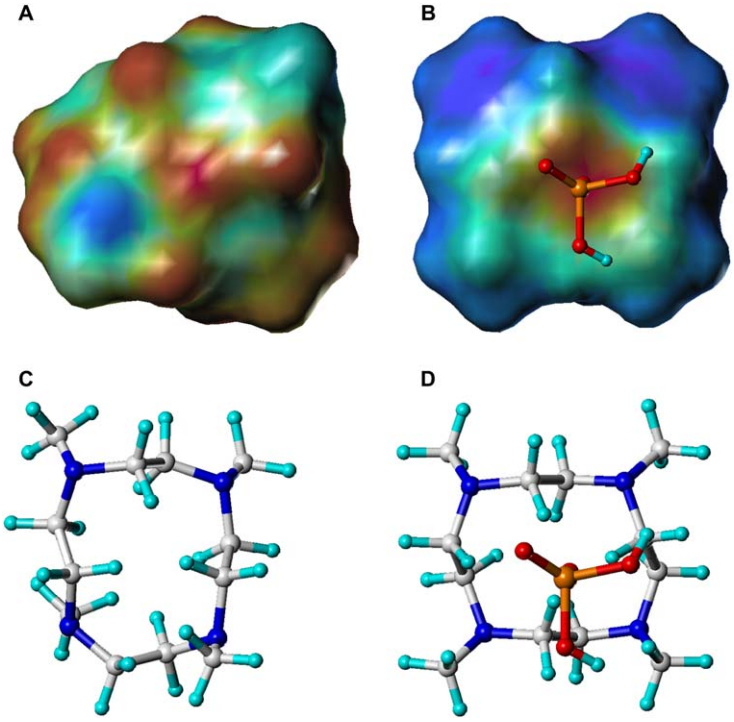

Figure 9. Electrostatic potential of **2** without (A) and with $H_2PO_4^-$ (B); in addition conformations of **2** without (C) and with $H_2PO_4^-$ (D) are given—instead of benzyl only R=Me was considered.

3. Conclusions

From the detailed NMR study of a series of aza crown ethers **1**–**10** both the stoichiometry and complex stability constants with the anions $H_2PO_4^-$ and HSO_4^- were obtained. The aza crown ethers generally form 1:1 complexes but the complex stability proved to be strongly dependent on the sterically hindering effect of the *N*-substituents if present. At the same time, the flexibility of **1**–**10** is reduced upon complexation.

Although structural *J* and spatial NOE information from NMR were very limited except in the case of **10**, the data were still able to be included as constraints in the accompanying molecular modeling study. As the major results of the modeling study it was determined that:

(i) *N*-Unsubstituted aza crown ethers prefer stable *endo* orientations of the donor atoms; if benzyl or alkyl substituents are present, due to their steric effects, donor atoms change *synclinal* to *antiperiplanar* orientations of N–C–C–N moieties.

(ii) *N*-Unsubstituted aza crown ethers form hydrogen bonds NH···O=S(O=P) to the corresponding anions; thereby, the geometry of the macrocyclic ring system changes in order to maximize the number and possibilities of this hydrogen bonding.

(iii) Complexation of aza crown ethers and anions in *N*-substituted compounds proceeds via dipole–ion interactions. Due to impossible H-bonding [cf. (ii)] and due to steric hindrance of complexation by the *N*-substituents, the stability constants of the corresponding complexes drop accordingly.

It has been proved by study that detailed structural information about crown ethers in solution can be obtained (both in free and complexed state) not only as an substantial alternative to X-ray studies in the solid state but also as the only information if no useful crystals could be obtained.

4. Experimental

4.1. Syntheses

The di-, tri-, and tetraaza crown ethers **1**–**9** and the mixed dioxa,diaza crown ether **10** were synthesized according to literature procedures collected in Ref. 23. The reaction products were purified by column chromatography and both the structure and purity of the compounds were determined by ^{1}H and ^{13}C NMR spectroscopy and accurate mass measurements by ESIMS. The salts $H_2PO_4^-{}^+N(n\text{-}Bu)_4$ and $HSO_4^-{}^+N(n\text{-}Bu)_4$ for the complexation studies were purchased from Aldrich and NMR solvents from Chemotrade; all were used without further purification.

4.2. NMR spectroscopy

^{1}H and ^{13}C NMR spectra were recorded on Bruker Avance 500 or 300 NMR spectrometers using 5 mm probes operating at 500 and 300 MHz for ^{1}H, and 125 and 75 MHz for ^{13}C. For all measurements, $CDCl_3$ (for lower temperatures CD_2Cl_2) was employed as the solvent using TMS as an internal reference (=0 ppm for both nuclei). ^{31}P NMR spectra were calibrated externally (capillary) with 85% H_3PO_4 (=0 ppm). Signal assignment was performed at 298 K and utilized standard Bruker pulse sequences (^{1}H, ^{13}C, ^{31}P, COSY, HMQC, and HMBC).

For ^{1}H NMR spectra, the digital resolution was set to 16 data points per hertz and to 1.6 data points per hertz for ^{13}C spectra. For 2D NOESY experiments, an optimal value for the mixing time τ_m was assessed as 400 ms. To avoid confusion arising from spin diffusion, 2D ROESY spectra were also recorded for comparison and also utilized mixing times of 400 ms. For both NOESY and ROESY experiments as well as the T_1 measurements, paramagnetic oxygen was displaced from the NMR solutions by ultrasonification for 30 min under argon prior to measurement. T_1 values were measured using the inversion recovery pulse sequence with a total of 16 different delay times. T_1 values were calculated using standard Bruker software and are reported with an uncertainty of 50 ms. Vicinal ^{1}H–^{1}H coupling constants were measured using the JRESQF pulse sequence where the spectral widths were set to 4125 and 40 Hz for the f_2 and f_1 dimensions, respectively, with digital resolutions of 4 and 0.2 Hz.

For the determination of the barriers to ring interconversion ($\Delta G^{\neq}$), the rate constants k_c at the coalescence temperatures T_c were calculated from the chemical sift difference $\Delta\nu$ of the respective peaks extrapolated to T_c using the Gutowski–Holm method ($k_c=2.22\times\Delta\nu$).[24] Inserting the resulting rate constants into the Eyring equation [$\Delta G^{\neq}=19.14\times T_c\times(10.32+\log(T_c/k_c)$] provided values of $\Delta G^{\neq}$. Coalescence temperatures are reported with an uncertainty of 1 K.

Titration experiments were conducted using the continuous variation method[25] as follows: stock solutions of the salts $H_2PO_4^-{}^+N(n\text{-}Bu)_4$ and $HSO_4^-{}^+N(n\text{-}Bu)_4$ and compounds **1**–**10** were, for ease of convenience, made to the same concentration (3.3×10^{-4} M) to facilitate a simple procedure whereby the sum of the concentrations of the ligands and the anions were maintained as a constant during the course of the titration. The ^{1}H NMR spectra of the free ligands were first recorded and then the concentration of the ligand was decreased successively whilst the concentration of the anion was increased accordingly (e.g., from **1**:$H_2PO_4^-{}^+N(n\text{-}Bu)_4$ or $HSO_4^-{}^+N(n\text{-}Bu)_4$=9:1 to 8:2…1:9, etc.).

4.3. Molecular modeling

Random search simulations were performed using the program *SYBYL*[21] with the Tripos force field[26] and consisted of 100,000 cycles. All torsional angles within the ring were allowed to vary randomly and no constraints were applied. After each cycle, the optimized conformation was stored if the heat of formation was within 3 kcal/mol of the lowest calculated heat of formation. The simulation was terminated prematurely if all so obtained conformations had been counted at least five times. This ensured that the global minimum was found with a confidence in excess of 95%.

Geometry optimizations were performed using the semiempirical method PM3.[27] The SCRF/SCIPCM (self-consistent reaction field/self-consistent isodensity polarized continuum model)[28] method were used to consider the solvent effect; the dielectric constant of chloroform (ε=4.8) was applied. Calculations were performed on IRIS-INDIGO XS24 or SGI O2 workstations or on PCs with Pentium 1 processors.

Acknowledgements

Synthesis of the compounds by Dr. Michael Gäbler (Synthon GmbH) and language correction of the manuscript by Dr. Karel D. Klika are gratefully acknowledged.

References and notes

1. Hosseini, M. W.; Lehn, J.-M. *Helv. Chim. Acta* **1987**, *70*, 1312.
2. (a) Mertes, M. P.; Mertes, K. B. *Acc. Chem. Res.* **1990**, *23*, 413; (b) *Supramolecular Chemistry of Anions*; Bianchi, A., Bowman-James, K., Garcia-España, E., Eds.; VCH: Weinheim, 1997; (c) Schmidtchen, F. P.; Berger, M. *Chem. Rev.* **1997**, *97*, 1609; (d) Shestakova, A. K.; Chertkov, V. A.; Schneider, H. J.; Lysenko, K. A. *Org. Lett.* **2001**, *3*, 325 and references therein.
3. (a) Xavier, C.; Paulo, A.; Domingos, A.; Santos, I. *Eur. J. Inorg. Chem.* **2004**, *2*, 243; (b) Subat, M.; Borovik, A.; König, B. *J. Am. Chem. Soc.* **2004**, *126*, 3185.
4. Chupakhin, O. N.; Itsikson, N. A.; Morzherin, Y. Y.; Charushin, V. N. *Heterocycles* **2005**, *66*, 689.
5. Llinares, J. M.; Powell, D.; Bowman-James, K. *Coord. Chem. Rev.* **2003**, *240*, 57.
6. Novak, I.; Potts, A. W. *J. Org. Chem.* **1996**, *61*, 786.
7. Ranganathan, R. S.; Pillai, R. K.; Raju, N.; Fan, H.; Nguyen, N.; Tweedle, M. F.; Desreux, J. F.; Jaques, V. *Inorg. Chem.* **2002**, *41*, 4846.

8. Bultinck, P.; van Alsenoy, C.; Goeminne, A.; van de Vondel, D. *J. Phys. Chem. A* **2000**, *140*, 11801.
9. Andres, A.; Arago, J.; Bencini, A.; Bianchi, A.; Domenech, A.; Fusi, V.; Garcia-Espania, E.; Paoletti, P.; Ramirez, J. A. *Inorg. Chem.* **1993**, *32*, 3418.
10. (a) Job, P. *Comp. Rend.* **1925**, *180*, 928; (b) Job, P. *Ann. Chim. Phys.* **1928**, *9*, 113.
11. Valiyaveettil, S.; Engbersen, J. F. J.; Verboom, W.; Reinhoudt, D. N. *Angew. Chem., Int. Ed. Engl.* **1993**, *32*, 900.
12. Martell, A. E.; Motekaitis, R. J.; Lu, Q.; Nation, D. A. *Polyhedron* **1999**, *18*, 3203.
13. Starke, I.; Kleinpeter, E, unpublished results.
14. Pihlaja, K.; Kleinpeter, E. *Carbon-13 NMR Chemical Shifts in Structural and Stereochemical Analysis*; Marchand, A. P., Ed.; Methods in Stereochemical Analysis; VCH: New York, NY, 1994; p 207.
15. (a) Holzberger, A.; Holdt, H.-J.; Kleinpeter, E. *Org. Biomol. Chem.* **2004**, *2*, 1691; (b) Holzberger, A.; Holdt, H.-J.; Kleinpeter, E. *J. Phys. Org. Chem.* **2004**, *17*, 257; (c) Holzberger, A.; Kleinpeter, E. *Magn. Reson. Chem.* **2004**, *42*, 589; (d) Kleinpeter, E.; Grotjahn, M.; Klika, K. D.; Drexler, H.-J.; Holdt, H.-J. *J. Chem. Soc., Perkin Trans. 2* **2001**, 988; (e) Kleinpeter, E. *J. Prakt. Chem.* **1991**, *333*, 817.
16. Wolf, R. E.; Hartmann, J. A. R.; Storey, J. M. E.; Foxman, B. M.; Cooper, S. R. *J. Am. Chem. Soc.* **1987**, *109*, 4328.
17. Lu, Q.; Motakaitis, R. J.; Reibenspies, J. J.; Martell, A. E. *Inorg. Chem.* **1995**, *34*, 4958.
18. Albelda, M. T.; Burguete, M. I.; Frias, J. C.; Garcie-Espana, E.; Luis, S. V.; Miravet, J. F.; Querol, M. *J. Org. Chem.* **2001**, *66*, 7505.
19. Beer, P. D.; Gale, P. A. *Angew. Chem., Int. Ed.* **2001**, *40*, 486.
20. (a) Connolly, M. L. *Science* **1983**, *221*, 709; (b) Connolly, M. L. *J. Appl. Crystallogr.* **1983**, *16*, 548.
21. (a) SYBYL Molecular Modeling Software, Version 6.8. Tripos: St. Louis, MO, 2003; (b) SYBYL Molecular Modeling Software. *Force Field Manual*, Version 6.8. Tripos: St. Louis, MO, 2003; pp 92–93; (c) SYBYL Molecular Modeling Software. *Molecular Spreadsheet Manual*, Version 6.8. Tripos: St. Louis, MO, 2003; pp 199–202; (d) SYBYL Molecular Modeling Software. *Graphics Manual*, Version 6.8. Tripos: St. Louis, MO, 2003; pp 199–202.
22. Gilson, M.; Sharp, K.; Honig, B. *J. Comput. Chem.* **1987**, *9*, 327.
23. Gokel, G. W. *Crown Ethers and Cryptands*; Stoddart, J. F., Ed.; Monographs in Supramolecular Chemistry; The Royal Society of Chemistry: Cambridge, 1991.
24. Gutowski, H. S.; Holm, C. H. *J. Chem. Phys.* **1956**, *25*, 1228.
25. (a) Shibata, Y.; Inouye, B.; Nakatsuka, Y. *Nippon Kagaku Kaishi* **1921**, *42*, 983; (b) Tsuchida, R. *Bull. Chem. Soc. Jpn.* **1935**, *10*, 27.
26. Clark, M.; Cramer, R. D., III; van Opdenbosch, N. *J. Comput. Chem.* **1989**, *10*, 982.
27. Stewart, J. J. P. *J. Comput. Chem.* **1989**, *10*, 209.
28. Foresman, J. B.; Keith, T. A.; Wiberg, K. B.; Snoonian, J.; Frisch, M. J. *J. Phys. Chem.* **1996**, *100*, 16098.